Human Papilloma Virus does not fully inactivate p53 in HNSCC

Jovanka Gencel-Augusto[1,2,*], Hua Li[1,2], Liam C. Woerner[1,2], Ashir A. Borah[2], Jeffrey N. Myers[3], Daniel E. Johnson[1,2], Jennifer R. Grandis[1,2]

[1]Department of Otolaryngology-Head and Neck Surgery, University of California San Francisco (UCSF), San Francisco, CA, USA. [2] UCSF Helen Diller Family Comprehensive Cancer Center, San Francisco, CA, USA. [3]Department of Head and Neck Surgery, MD Anderson Cancer Center, Houston, TX, USA. *Correspondence: jovanka.gencelaugusto@ucsf.edu

Abstract

Head and neck squamous cell carcinoma (HNSCC) is a major global health challenge. Inactivation of the tumor suppressor p53 is the most frequent molecular event in this malignancy. p53 inactivation occurs either through *TP53* mutations in HPV-negative cases or via HPV-mediated p53 degradation in HPV-positive (HPV+) cases, where most retain a wild-type (WT) *TP53* allele. This underscores the critical role of p53-regulated processes in HNSCC pathogenesis. Clinically, HPV+ HNSCC is associated with significantly better outcomes than HPV-negative cases. Despite HPV E6-mediated degradation of p53, 10% of HPV+ HNSCC cases have mutant *TP53* alleles, suggesting an additional need to suppress p53 signaling. In this study, we demonstrate that HPV+ *TP53*-WT HNSCC cells have residual p53 activity, with tumor-suppressive effects. Specifically, ablation of p53 in HPV+ *TP53*-WT HNSCC cells lead to increased proliferation, migration, and invasion. RNA-sequencing revealed that p53 regulates gene transcription (both activation and repression) in the presence of HPV, and we confirmed that these functions are p53-specific. Human tumor data further reveal that among HPV+ HNSCC cases, those with WT *TP53* have significantly better survival outcomes than HPV+ cases with *TP53* mutations. Notably, HPV+ *TP53*-WT HNSCC tumors show decreased PI3K-AKT signaling, increased gene methylation in oncogenic pathways, and fewer chromosomal alterations compared to HPV+ *TP53*-mutant tumors. These findings challenge the prevailing notion that p53 is entirely inactivated in HPV+ HNSCC and provide critical insights into HNSCC-specific, p53-driven tumor suppression mechanisms with implications for targeted therapies in HNSCC.

Introduction

Head and neck squamous cell carcinoma (HNSCC) represents a significant global health challenge, with approximately 900,000 new cases diagnosed annually [1]. Nearly all cases involve inactivation of p53, a key regulator of anti-tumor responses. In ~70% of cases, p53 inactivation occurs through genetic alterations in *TP53*, while ~20% result from human papillomavirus (HPV) infection, which promotes constitutive degradation of the p53 protein (HPV-positive, HPV+) [2]. This underscores the central role of p53-regulated pathways in HNSCC pathogenesis. Clinically, *TP53* mutations in HNSCC are associated with poor response to conventional therapies and significantly worse survival outcomes [3]. Despite extensive efforts, no effective treatments exist for the vast majority of *TP53*-mutant cancers, largely due to the challenge of selectively targeting mutant p53 proteins, which are often deemed "undruggable" . In contrast, HPV+ HNSCC, which in 90% of cases retain wild-type (WT) *TP53* alleles but experience HPV-mediated p53 degradation, exhibits markedly better prognosis [2, 4] (Supplementary Figure 1) and therapeutic responsiveness than HPV-negative (mostly *TP53*-mutant) HNSCC [2]. The molecular determinants for these differences are not well understood.

p53 functions as a transcription factor, orchestrating the expression of hundreds of genes (both up and down) involved in apoptosis, cell cycle arrest, senescence, and several other processes, to suppress tumor development [5]. HPV promotes p53 degradation through the viral E6 protein, which hijacks the host E3 ubiquitin ligase E6AP, targeting p53 for proteasomal degradation [6]. This mechanism mirrors the cellular intrinsic regulation of p53 via MDM2 (Supplementary Figure 1), another E3 ubiquitin ligase that both tags p53 for degradation and directly inhibits its transcriptional activity by binding to the p53 transcriptional activation domain [7]. Notably, p53 transcriptionally activates *MDM2*, establishing a tightly regulated feedback loop that restrains excessive p53 activity [7], which could otherwise be detrimental to normal cells.

Seminal studies have demonstrated that MDM2-mediated regulation of p53 signaling is essential for maintaining organismal homeostasis. Genetic deletion of *Mdm2* in mice results in p53-dependent embryonic lethality [8]. Similarly, conditional deletion of *Mdm2* in adult murine tissues triggers robust activation of p53 target genes that result in severe multi-organ toxicities - phenotypes that are rescued by *p53* deletion [9]. This evidence underscores the key role of MDM2 in regulating p53 activity to prevent irreversible cellular outcomes. Consequently, under homeostatic conditions, healthy tissues maintain very low p53 protein levels due to MDM2-driven degradation. However, low p53 protein abundance does not equate to a complete absence of p53 signaling [10]. Beyond the well-characterized roles of p53 in acute responses to cellular stressors such as DNA damage or oncogene activation (i.e. apoptosis, cell cycle arrest), it also performs essential homeostatic functions. These functions include preserving mesenchymal stem cell integrity [11], regulating airway epithelial differentiation [12, 13], modulating cellular metabolism [14, 15], among other fundamental processes that contribute to organismal function and tumor suppression.

Taking these data together, including documented p53 functions at low protein levels and the molecular and clinical characteristics of HPV+ HNSCC, we hypothesized that HPV+ *TP53*-WT HNSCC retains residual p53 tumor suppressive signaling.

To investigate this, we utilized a panel of HPV+ p53-WT HNSCC cell lines with or without p53 ablation and performed downstream assays. Surprisingly, further downregulation of p53 through RNA interference in HPV+ HNSCC cells resulted in more aggressive cellular phenotypes, suggesting that residual p53 activity constrains tumor progression in the presence of HPV. RNA sequencing revealed p53-driven transcriptional regulation of multiple genes both up and down. Several of these genes are also differentially expressed upon ectopic WT p53 expression in HPV-negative HNSCC cells, reinforcing that the observed phenotypes in HPV+ HNSCC are specifically p53-driven. Lastly, stratification of HPV+ HNSCC cases by *TP53* status reveals that HPV+ *TP53*-WT cases have

significantly better survival outcomes than their HPV+ *TP53*-mutant cases. HPV+ *TP53*-WT HNSCC tumors exhibit increased gene methylation in oncogenic pathways, decreased PI3K-AKT signaling, and fewer chromosomal alterations compared to HPV+ *TP53*-mutant tumors.

This study provides evidence of a residual tumor-suppressive program driven by p53 in HPV+ HNSCC, challenging the prevailing notion that p53 is completely inactivated by HPV. Our findings suggest that this retained activity may contribute to the differential clinical outcomes between HPV+ and HPV- HNSCC and that stratification of HPV+ HNSCC cases by *TP53* status could improve responses to current therapies. Furthermore, we propose that HPV+ HNSCC models serve as a unique platform to study disease-specific p53-driven tumor suppression mechanisms that may inform novel therapeutic strategies for *TP53*-mutant cancers.

Results

p53 inhibits HNSCC cell proliferation, migration, and invasion in the presence of HPV

We first investigated the functional consequences of p53 ablation in *TP53*-WT HPV+ HNSCC cell lines using siRNA-mediated p53 knockdown, with a non-targeting siRNA as a control. To assess the impact of p53 loss, we examined cell proliferation, migration, and invasion.

p53 siRNA effectively reduced p53 mRNA and protein levels compared to a non-targeting control siRNA at the assessed time points (Supplementary Figures 2, 4). p53 knockdown significantly enhanced proliferation in UM-SCC-47 (Figure 1A) as well as in UPCI-SCC-090 and UD-SCC-2 (Supplementary Figure 2). Additionally, in UM-SCC-47, p53 depletion increased both migration and invasion capabilities (Figure 1B-C). UPCI-SCC-090 and UD-SCC-2 did not exhibit baseline migration or invasion, preventing assessment of these processes upon p53 knockdown.

These findings suggest that WT p53 activity present in HPV+ HNSCC cells mitigates tumor cell progression, highlighting a potential tumor-suppressive role despite HPV-mediated p53 degradation.

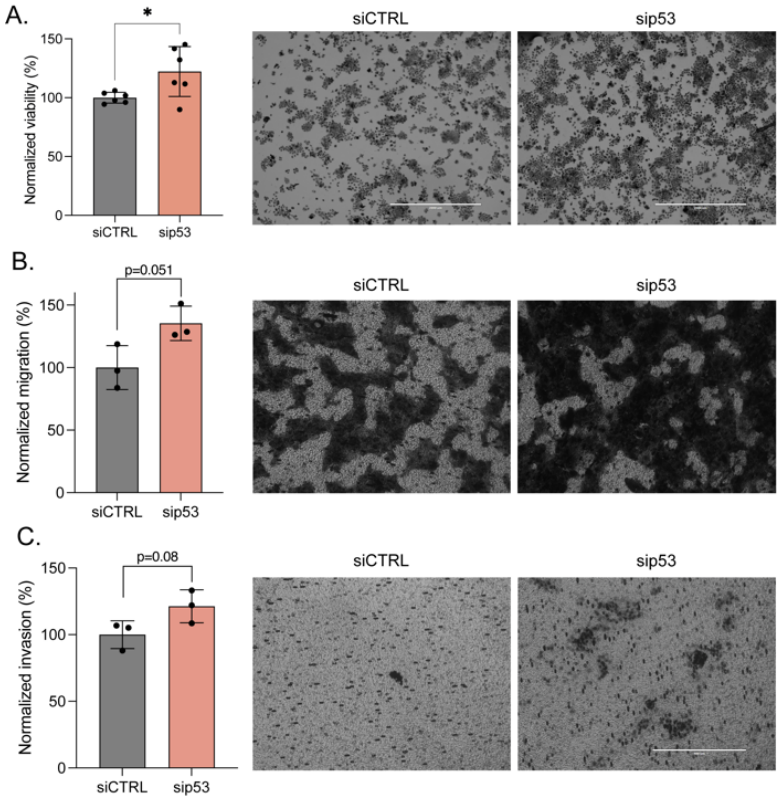

Figure 1.- WT p53 ablation increases proliferation, migration, and invasion in HPV+ HNSCC cells. A. Viability assay following *p53* knockdown (48h, UM-SCC-47), *p<0.05. Migration **(B)** and invasion **(C)** assays in UM-SCC-47 following *p53* knockdown (48 hours). Representative end point images are presented to the right of the corresponding bar plots.

p53 drives residual transcriptional regulation in the presence of HPV

Given the phenotypic consequences of p53 ablation in HPV+ HNSCC cells, we hypothesized that p53 transcriptional activity is retained. To investigate this, we performed RNA-sequencing following p53 knockdown in two HPV+ *TP53*-WT HNSCC cell lines, UM-SCC-47 and UPCI-SCC-090, using a non-targeting siRNA as a control. Samples were collected 30 hours post-transfection, a time point selected based on the kinetics of *CDKN1A* (p21, a canonical p53 target gene) expression changes observed at 8, 12, 24, 30, and 48 hours post-transfection (Supplementary Figure 3). Across all time points, *CDKN1A* levels were significantly reduced upon p53 knockdown, with the most pronounced effect at 30 and 48 hours. We selected 30 hours to minimize the influence of compensatory signaling that is not p53-dependent.

Differential gene expression analysis revealed many differentially expressed genes (DEGs; $p<0.01$; $|Log_2 fold\text{-}change| > 0$) following p53 knockdown in both cell lines (Figure 2A-B). Among the identified DEGs, ~60% were downregulated and ~40% were upregulated. To determine whether these DEGs include direct p53 targets, we compared our DEG lists with previously identified p53-bound genes from p53 chromatin immunoprecipitation sequencing (ChIP-seq) datasets [16]. Approximately 20% of the DEGs in each cell line overlapped with known direct p53 targets (Figure 2C, top). These findings are consistent with previous reports of p53 as both transcriptional activator and repressor [17]. However, the total number of DEGs was markedly lower than what has been reported in HPV-negative contexts and other cell types, either following *Mdm2* genetic deletion [18] or in response to DNA damage-induced p53 activation [16]. This suggests that while p53 functionality is restricted in HPV+ HNSCC, it remains present.

We further analyzed DEGs shared between the two HPV+ HNSCC cell lines and identified 16 common genes (Figure 2C, bottom), of which 13 were downregulated upon p53 knockdown, indicating p53-

dependent activation (Figure 2D). Among these downregulated genes were *CDKN1A* (p21), *INPP5D*, and *GDF15* all well-established tumor-suppressors [19, 20]. Conversely, two of the three shared upregulated genes upon p53 knockdown, *RRM2* and *NCEH1*, have been previously described as tumor-promoting [21, 22]. Collectively, these shared DEGs regulate diverse cellular processes, including cell cycle progression, inflammation, lipid metabolism, cell motility, endoplasmic reticulum (ER) stress, iron metabolism, and cysteine metabolism (Figure 2D).

Consistent with the RNA-based findings, we confirmed that p21 protein was downregulated following p53 knockdown, persisting at 48 and 72 hours post-transfection. Similarly, CDK1, a key regulator of cell cycle progression, was upregulated at both time points (Figure 2E).

Taken together, these findings demonstrate that WT p53 maintains a residual transcriptional program in HPV+ HNSCC, regulating genes involved in tumor suppression and cellular homeostasis despite HPV-mediated degradation.

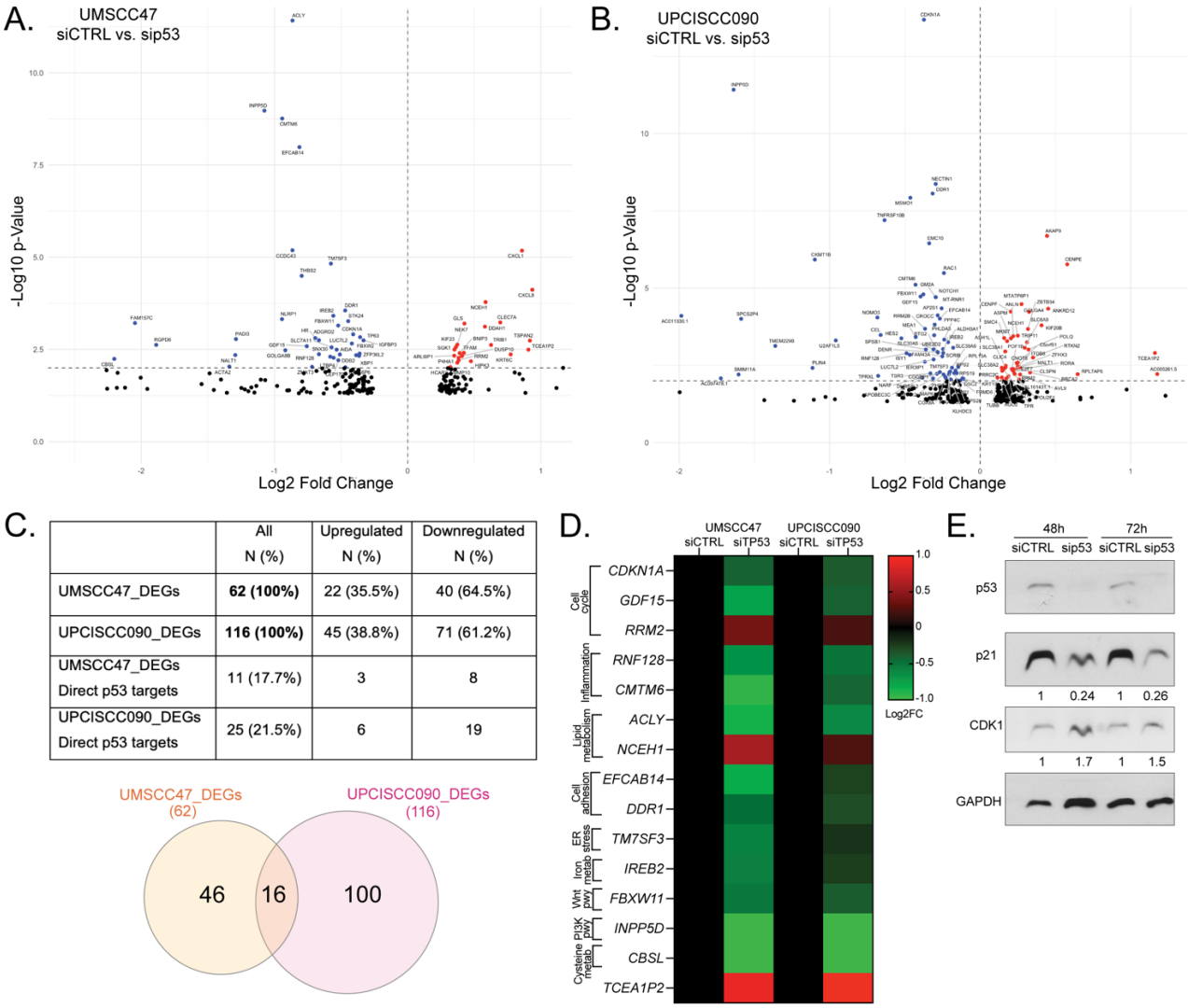

	All N (%)	Upregulated N (%)	Downregulated N (%)
UMSCC47_DEGs	**62 (100%)**	22 (35.5%)	40 (64.5%)
UPCISCC090_DEGs	**116 (100%)**	45 (38.8%)	71 (61.2%)
UMSCC47_DEGs Direct p53 targets	11 (17.7%)	3	8
UPCISCC090_DEGs Direct p53 targets	25 (21.5%)	6	19

Figure 2. p53 regulates gene expression in the presence of HPV. A. Volcano plot shows significant differentially expressed genes (DEGs, blue=downregulated, red=upregulated, p<0.01) in UM-SCC-47 upon *p53* knockdown (two biological replicates per experimental condition). **B.** Volcano plot for DEGs in UPCI-SCC-090 upon *p53* knockdown (two biological replicates per experimental condition). **C. Top:** Table shows a summary of total, upregulated, or downregulated DEGs per cell line, including number of genes that are previously reported as direct p53 targets ("p53-bound") [16]. **Bottom:** Venn diagram shows shared and cell line-specific DEGs in UMSCC47 and UPCISCC090. **D.** Heatmap illustrates expression levels of shared DEGs in both cell lines. Green shades indicate downregulated genes, while red shades indicate upregulated genes. Values are represented as Log2 fold-change (Log2FC), with those exceeding |1| capped at +1 or -1 for illustrative clarity. Rows are genes and columns are experimental conditions. The cellular processes related to each gene are shown on the left. Pwy=pathway, Metab=metabolism. *TCEA1P2* is a pseudo-gene with no known function. **E.** Validation of protein changes, including p53 knockdown, p21 (*CDKN1A*) downregulation, and CDK1 upregulation in UM-SCC-47 at 48 and 72 hours post-transfection. Quantification of blots is shown relative to GAPDH and to siCTRL samples per time point.

p53 transcriptional regulation in HPV+ HNSCC is p53-specific

To validate that the observed transcriptional changes result from p53-driven regulation, we first restored p53 protein levels by knocking down E6 (Supplemental Figure 4). This approach effectively rescued the expression of p53 targets *CDKN1A* and *INPP5D* (Figure 3A).

To further confirm that these transcriptional effects are p53-dependent and not exclusive to HPV+ cells, we examined the expression of these genes in an HPV-negative context. We utilized PCI-13 HNSCC cell lines (harboring a spontaneous *TP53* deletion) that stably express ectopic *TP53*-WT or *TP53*-mutant (p53G245D) sequences [23]. Normalized read counts from RNA-sequencing analysis in these cell lines showed significantly higher expression levels of *CDKN1A*, *INPP5D*, *GDF15*, *ACLY*, *RNF128*, and *TM7SF3* in HPV-negative PCI-13 cells expressing WT p53 compared to their p53-mutant counterparts (Figure 3B).

These findings confirm that the transcriptional changes observed in HPV+ HNSCC cells (Figure 2) are specifically driven by p53.

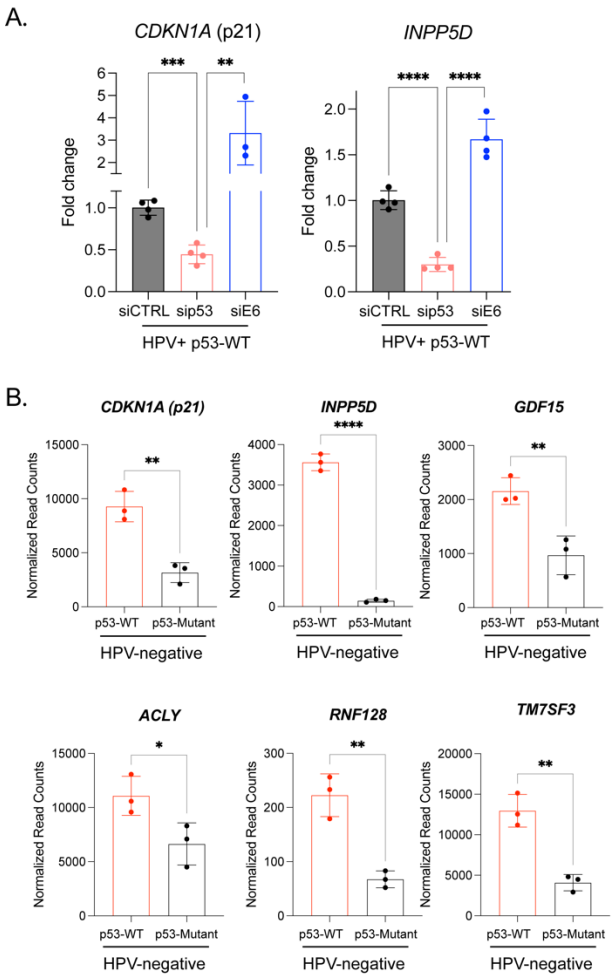

Figure 3.- p53 transcriptional regulation in HPV+ HNSCC is p53-specific. A. mRNA expression levels of p53 target genes *CDKN1A* and *INPP5D* decrease upon p53 knockdown and are restored (and elevated) following E6 knockdown in HPV+ HNSCC cells. **B.** Normalized RNA-seq read counts for *CDKN1A, INPP5D, GDF15, ACLY, RNF128, TM7SF3* in isogenic HPV-negative PCI-13 HNSCC cell lines with either WT p53 or G245D p53 mutant expression.

Human tumor data reveal significant clinical and molecular differences between HPV+ p53-WT and HPV+ p53-mutant HNSCC

Based on our experimental findings suggesting tumor-suppressive signaling in HPV+ HNSCC cells that retain WT *TP53* alleles, we analyzed human tumor data. We stratified HPV+ HNSCC tumors from The Cancer Genome Atlas (TCGA) by *TP53* status (WT vs. mutant) and assessed clinical outcomes. Notably, HPV+ *TP53*-WT tumors exhibited significantly better progression-free survival than *TP53*-mutant cases (Figure 4A).

Despite the lower prevalence of *TP53* mutations in HPV+ HNSCC, we also identified several statistically significant molecular differences between *TP53*-WT (n=64) and *TP53*-mutant (n=7) HPV+ tumors. One of the p53 target genes identified earlier (Figures 2-3), *INPP5D*, encodes a phosphatase that converts PIP3 to PIP2, thereby inhibiting PI3K-AKT signaling. We found *INPP5D* to be significantly upregulated in HPV+ *TP53*-WT tumors (Figure 4B), suggesting a potential role for p53 in suppressing PI3K-AKT signaling.

Further supporting this, we observed significantly increased *MYC* and *CCND1* mRNA levels - markers of AKT activation - in HPV+ *TP53*-mutant tumors (Figure 4B). Moreover, knockdown of WT p53 in the HPV+ HNSCC cell line UPCI-SCC-090 led to increased p110-alpha expression (PI3K catalytic subunit), indicative of PI3K pathway activation in the absence of WT p53 in HPV+ HNSCC (Figure 4C).

Together, these findings suggest that WT p53 in HPV+ HNSCC may suppress PI3K signaling via *INPP5D* transactivation and p110-alpha inhibition (Figure 4D).

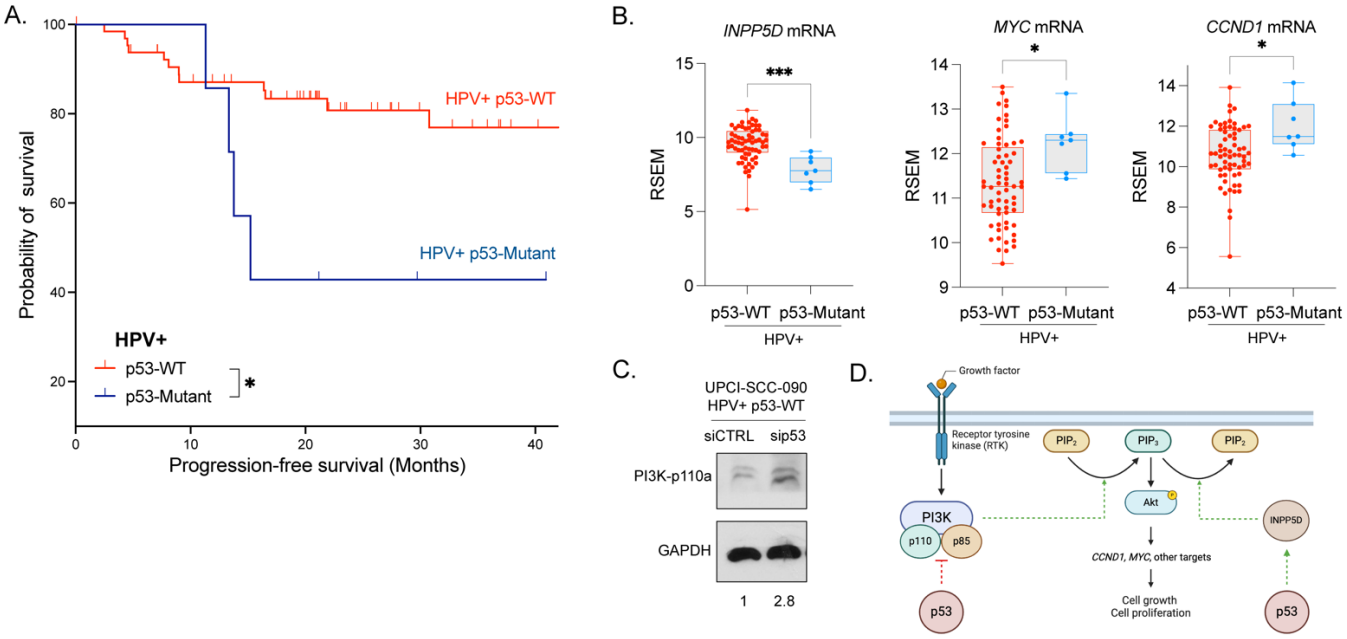

Figure 4. HPV+ *TP53*-WT HNSCC cases exhibit better clinical outcomes and suppression of PI3K signaling. A. Progression-free survival analysis comparing HPV+ *TP53*-WT and HPV+ *TP53*-Mutant HNSCC cases. *p < 0.05. **B.** Normalized RNA-seq read counts (RSEM) for *INPP5D, MYC,* and *CCND1* in HPV+ *TP53*-WT and HPV+ *TP53*-Mutant HNSCC tumors. **C.** Immunoblot analysis of PI3K-p110α and GAPDH in UPCI-SCC-090 cells 48 hours post-transfection with siRNA targeting p53 (sip53) or a non-targeting control (siCTRL). Blot quantification is shown relative to GAPDH and siCTRL. **D.** Schematic representation of p53-mediated inhibition of the PI3K-AKT pathway in HPV+ HNSCC.

We further analyzed global RNA expression differences between *TP53*-WT and *TP53*-Mutant HPV+ HNSCC tumors (Supplementary Figure 5). Pathway enrichment analysis revealed that *TP53*-Mutant tumors exhibit upregulation of genes associated with cell growth processes, including epithelial development, tissue morphogenesis, WNT signaling, and anabolic metabolism. In contrast, *TP53*-WT tumors showed increased expression of genes involved in immune regulation, DNA repair, and catabolic metabolism, among other processes. These data further reinforce our findings that p53 exerts tumor-suppressive functions in the presence of HPV in HNSCC.

In addition to gene expression differences, we also observed differential DNA methylation patterns between HPV+ *TP53*-WT and HPV+ *TP53*-Mutant tumors. These data were obtained from the HM27 and HM450 arrays, DNA methylation profiling platforms available in cBioPortal for assessing epigenetic alterations in cancer. These arrays cover CpG methylation in promoter, enhancer, and gene body regions, and identify methylation-driven gene silencing. We found that *TP53*-WT tumors exhibited significantly higher overall gene methylation compared to *TP53*-Mutant tumors. Specifically, *TP53*-Mutant tumors showed significantly increased methylation in only 23 genes, whereas *TP53*-WT tumors displayed elevated methylation across more than 500 genes (Figure 5A). Pathway enrichment analysis revealed that methylated genes in *TP53*-Mutant tumors were predominantly associated with tumor-suppressive pathways, while methylated genes in *TP53*-WT tumors were linked to tumor-promoting pathways (Figure 5A).

To determine whether differential methylation correlated with gene expression, we examined key oncogenes and tumor suppressors. *MET*, an oncogene, exhibited significantly higher methylation in *TP53*-WT tumors, which corresponded to lower *MET* mRNA expression (Figure 5B). Conversely, *VHL* and *PIK3R1*, both tumor suppressors, showed significantly lower methylation levels and higher mRNA expression in *TP53*-WT tumors (Figure 5B). These findings highlight the potential regulatory role of p53

in shaping the epigenetic landscape of HPV+ HNSCC tumors, influencing both oncogene suppression and tumor suppressor activation.

Lastly, given the role of p53 in maintaining genome integrity and our observation of significant upregulation of DNA repair pathway genes in *TP53*-WT HPV+ HNSCC tumors (Supplementary Figure 5), we investigated the incidence of chromosomal alterations in *TP53*-WT vs. *TP53*-Mutant HPV+ HNSCC tumors (Figure 5). We identified significant differences in 11 genomic loci, with 10 of them exhibiting a higher frequency of alterations in *TP53*-Mutant tumors. On average, fewer than 20% of *TP53*-WT tumors displayed chromosomal abnormalities, whereas over 40% of *TP53*-Mutant tumors exhibited such alterations. These findings further support a role for WT p53 in preserving genomic stability in HPV+ HNSCC.

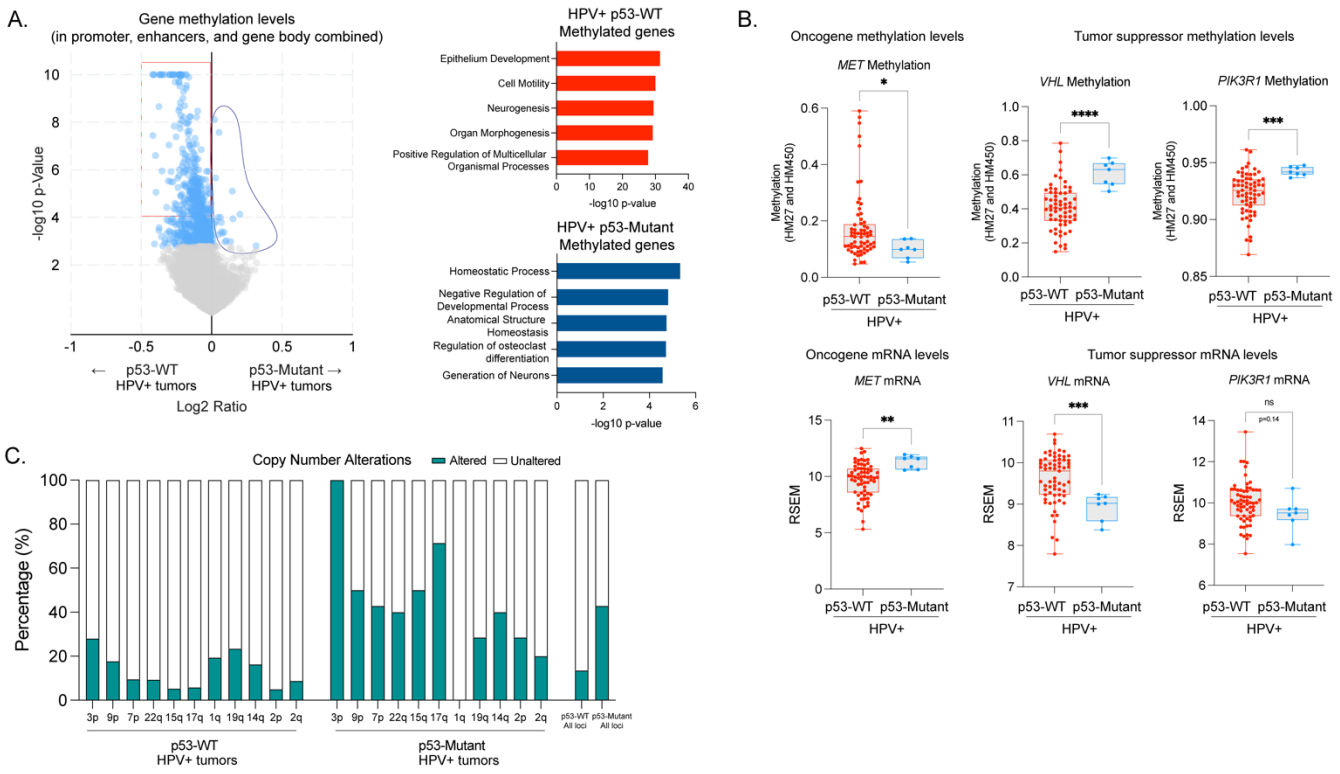

Figure 5.- HPV+ p53-WT HNSCC tumors exhibit higher gene methylation levels and fewer chromosomal abnormalities compared to HPV+ p53-Mutant tumors. A. Differential gene methylation is presented as $\log_2$ fold change ($\log_2$Ratio). In the volcano plot, significantly differentially methylated genes are highlighted in light blue. Genes with significantly higher methylation in *TP53*-WT tumors that were used for pathway enrichment analysis (500 genes) are outlined in red, while those with significantly higher methylation in *TP53*-Mutant tumors used for pathway analysis are outlined in blue (23 genes). Right panels display pathway enrichment analysis of differentially methylated genes for each tumor type, based on the Gene Ontology Biological Process (GOBP) dataset. **B.** Normalized methylation levels (top row) and RNA-seq read counts (RSEM) (bottom row) for *MET, VHL,* and *PIK3R1* in HPV+ *TP53*-WT and HPV+ *TP53*-Mutant HNSCC tumors. Statistical significance is indicated as follows: *p<0.05, **p<0.005, ***p<0.0005, ****p<0.00005, ns=not significant. **C.** Chromosomal alterations (gains and losses) across specified loci. The Y-axis represents the percentage of tumors with chromosomal alterations, while the X-axis denotes the specific genomic loci analyzed.

`

Discussion

HPV+ HNSCC exhibits distinct clinical behavior and significantly better outcomes compared to HPV-negative HNSCC [4]. A seminal discovery in 1990 revealed that HPV16 and HPV18-encoded E6 proteins promote p53 degradation [24]. Subsequent studies have shown that HPV may also impair p53 transcriptional activity [25]. These HPV-driven mechanisms of p53 inhibition parallel the physiological regulation of p53 by MDM2. Despite MDM2-mediated inhibition, p53 maintains homeostatic signaling critical for various cellular processes including tumor suppression. Notably, while the majority of HPV+ HNSCC cases retain WT *TP53* alleles, 10% of cases harbor deactivating *TP53* mutations, suggesting a need to further dampen this pathway. Although it is well established that HPV suppresses p53 function, the extent of this suppression remains undefined. Here, we tested the hypothesis that WT p53 drives residual tumor suppressive activity in HPV+ HNSCC.

To assess this, we further inhibited p53 via siRNA in HPV+ *TP53*-WT HNSCC cell lines and conducted functional assays. Consistent with our hypothesis, p53 knockdown enhanced cell proliferation, migration, and invasion, suggesting that residual p53 activity suppresses tumor-promoting phenotypes even in the presence of HPV. Furthermore, transcriptomic analyses revealed that p53 continues to regulate gene expression, activating tumor suppressor genes while repressing tumor-promoting genes. Notably, besides regulation of the cell cycle, p53-regulated genes were enriched in pathways related to metabolism and inflammation. E6 knockdown effectively elevated expression of the p53 targets *CDKN1A* and *INPP5D*, suggesting that this is a p53-dependent phenotype. Using a pair of HPV-negative isogenic cell lines, we further demonstrated that many of the genes regulated by p53 in HPV+ cells are also regulated by p53 in the absence of HPV. These findings collectively support a model in which HPV suppresses but does not fully abolish p53 function.

To extend these findings to patient tumors, we analyzed HPV+ HNSCC cases stratified by *TP53* status and found that tumors retaining WT p53 were associated with significantly better survival. To investigate the molecular mechanisms underlying this survival advantage, we examined the expression of p53-regulated genes identified in our cell line models within HPV+ HNSCC tumors. Among 16 genes tested, *INPP5D* (SHIP1), a direct p53 target and known tumor suppressor, was the only gene significantly upregulated in *TP53*-WT vs. *TP53*-mutant HPV+ tumors. Because INPP5D negatively regulates the PI3K-AKT pathway, we investigated pathway activity and observed increased expression of *MYC* and *CCND1* in p53-mutant tumors, consistent with enhanced PI3K-AKT signaling. Supporting this, p110-alpha (the catalytic subunit of PI3K) was upregulated upon WT p53 knockdown in HPV+ HNSCC cells, further implicating p53 in modulating PI3K activity.

These findings have important implications as HPV+ HNSCC is generally resistant to PI3K-targeting therapies [26]. Our data provide a potential mechanistic explanation: residual WT p53 activity may partially suppress PI3K signaling, reducing cellular dependence on this pathway and thereby limiting the efficacy of PI3K inhibitors. In contrast, *TP53*-mutant HPV+ tumors, which exhibit upregulation of the PI3K-AKT pathway (potentially due to complete loss of p53 function), may remain sensitive to PI3K inhibition. This raises the hypothesis that stratifying HPV+ HNSCC patients by *TP53* status could improve treatment outcomes by identifying patients who are more likely to benefit from PI3K-targeted therapies. Future studies should explore whether *TP53*-mutant HPV+ tumors display increased sensitivity to PI3K inhibitors in clinical settings, potentially leading to more personalized treatment strategies.

Further investigation of the molecular features of HPV+ HNSCC tumors based on *TP53* status revealed a higher degree of gene methylation in *TP53*-WT cases compared to p53-mutant tumors. Notably, many of the hypermethylated (silenced) genes in *TP53*-WT tumors were tumor-promoting, including the oncogene *MET*, which correlated with lower *MET* mRNA expression in these tumors. Beyond

differences in methylation and gene expression, *TP53*-WT tumors also exhibited fewer chromosomal abnormalities.

These findings have significant clinical implications, highlighting distinct molecular subtypes within HPV+ HNSCC based on *TP53* status. While most HPV+ HNSCC cases are associated with favorable clinical outcomes, a subset displays aggressive behavior similar to HPV-negative tumors. One possible explanation for this aggressive subset is the presence of *TP53* mutations. Consequently, therapeutic strategies should not be uniform for all HPV+ HNSCC cases but rather tailored based on *TP53* status. For instance, MET inhibitors such as Cabozantinib may be more effective in *TP53*-mutant HPV+ HNSCC, where MET is more highly expressed, whereas *TP53*-WT HPV+ tumors may derive less benefit due to epigenetic silencing of *MET*. Additionally, whether residual p53 signaling contributes to the observed resistance of HPV+ HNSCC to Cetuximab, a widely used EGFR-targeting therapy, remains an open question. Similarly, the role of WT p53 in mediating responses to radiotherapy in HPV+ HNSCC warrants further investigation. Our data also suggest that WT p53 may modulate immune responses in HPV+ HNSCC (Figure 2, Supplementary Figure 5), highlighting the potential for stratifying immune checkpoint inhibitor (ICI) therapy by *TP53* status. Further molecular studies are needed to mechanistically define the role of p53 in these therapeutic responses.

Conclusion

Together, our findings reveal that p53 retains functional relevance in HPV+ HNSCC and may influence tumor behavior and therapeutic response. Understanding the molecular distinctions between *TP53*-WT and *TP53*-mutant HPV+ HNSCC could improve patient stratification and guide the development of more effective, precision-based treatments. Future studies should aim to elucidate how residual p53 activity modulates key oncogenic pathways and determine whether targeting these pathways can improve clinical outcomes in *TP53*-mutant HNSCC. Our findings suggest that HPV+ *TP53*-WT HNSCC

models provide a unique platform for uncovering disease-specific p53-driven tumor-suppressive functions, which could be pharmacologically restored in *TP53*-mutant HNSCC to enhance clinical outcomes.

Materials and Methods

Cell lines and cell culture

Human cell lines UM-SCC-47, UPCI-SCC-090 and UD-SCC-2 were selected from a panel of HPV+ HNSCC cell lines that have no endogenous *TP53* mutation as confirmed by the Broad Institute Cancer Cell Line Encyclopedia. These cells were maintained in Dulbecco's Modified Eagle's medium (Corning) supplemented with 10% fetal bovine serum, and 1% penicillin/streptomycin. Cells were maintained in a humidified incubator at 37°C and 5% carbon dioxide. Each cell line thawed and passaged approximately 3-4 times before necessary experimentation. Genotype authentication for human cell lines was performed by LabCorp using the STR method. Cell lines are routinely authenticated every 6 months with latest date 08/06/2024. Isogenic human *TP53* cell lines (p53WT and p53G245D) were obtained from the laboratory of Dr. Jeffrey N. Myers at The University of Texas MD Anderson Cancer Center and maintained as described previously [23].

Proliferation, Migration, and Invasion Assays

Proliferation: cells were seeded at approximately 10,000 cells per well in 48 well plates. 24 hours after seeding, cells were transfected with siRNA constructed to target p53 (Horizon Discovery, L-003329-00-0005) or non-targeting control (Horizon Discovery, D-001810-10-20) using Lipofectamine RNAiMAX (ThermoFisher, 13778075). Cells were incubated for 48 hours (UM-SCC-47 and UD-SCC-2) or 72 hours (UPCI-SCC-090) at 5% CO2 and 37 degrees. Crystal violet assay was performed as directed by manufacturer (Abcam Kit, ab232855).

Migration and Invasion: cells were seeded at 300,000 cells per well in 6-well plates. 24 hours after seeding, cells were transfected with siRNA constructed to target p53 (Horizon Discovery, L-003329-00-0005) or non-targeting control (Horizon Discovery, D-001810-10-20) using Lipofectamine RNAiMAX (ThermoFisher, 13778075). 24 hours after transfection, cells were harvested, counted, and re-seeded in FBS-free media in either 24-well Migration plates (polycarbonate membrane) or 24-well Invasion Chambers (basement membrane) (50,000 cells/well) as directed by the manufacturer (CellBioLabs INC, CBA-100-C). We used 10% FBS-supplemented growth media as attractant. Twenty hours later, we measured cell migration and invasion using the provided cell viability staining solution (CellBioLabs INC, CBA-100-C).

Immunoblotting

Cells were seeded at 300,000 cells per well in a 6-well plate. 24 hours after seeding, cells were transfected with siRNA constructed to target p53 (Horizon Discovery, L-003329-00-0005), E6 (Santa Cruz, sc-156008) or non-targeting control (Horizon Discovery, D-001810-10-20) using Lipofectamine RNAiMAX (ThermoFisher, 13778075). Cells were harvested at 24, 30, 48, or 72 hours post-transfection using cell lysis buffer (Cell Signaling Technology, Cat#9803 with cOmplete Protease Inhibitor Cocktail (Roche, Cat#11836170001). Protein concentration was determined using a Bradford Assay (Bio-Rad, Cat#5000006). Proteins were standardized to 100 ug/uL, diluted with cell lysis buffer. 30 ug of protein was electrophoresed on a 10% SDS-PAGE gel and transferred to a PVDF membrane (Bio-Rad, Cat#1620177) at 25V for 1 hour. Membranes were blocked in 5% nonfat dried milk (Apex Bioresearch, Cat#20-241) reconstituted in TBST (Teknova, Cat#T1680) for 15 minutes. Membranes were incubated in a 1:1000 concentration of primary antibodies overnight. Primary antibodies: GAPDH (D16H11) XP® Rabbit mAb (Cell Signaling Technology, Cat # 5174S), p53 (DO1) (Santa Cruz Biotechnology, Cat# sc-126), p21 Wafl/cipl (12D1) (Cell Signaling Technology, Cat# 2947S), CDK1/CDK2 (Santa Cruz Biotechnology, Cat# sc-53219), PI3K p110-alpha (Cell Signaling Technology, Cat# 4255). Membranes were incubated in 1:3000 concentration of secondary HRP- labeled antibody in 2.5% nonfat dried milk

for 2 hours. Membranes were developed using Luminol Reagent (Santa Cruz Biotechnology, Cat# sc-2048) and imaged using the Bio-Rad ChemiDoc Imaging system. ImageJ was used for densitometry analysis.

Quantitative RT-PCR

Cells were seeded at 300,000 cells per well in a 6-well plate. 24 hours after seeding, cells were transfected with siRNA constructed to target p53 (Horizon Discovery, L-003329-00-0005), E6 (Santa Cruz, sc-156008), or non-targeting control (Horizon Discovery, D-001810-10-20) using Lipofectamine RNAiMAX (ThermoFisher, 13778075). Cells were harvested at 8, 12, 24, 30, or 48 hours post-transfection, and RNA was isolated using the Direct-zol RNA MiniPrep with TRIReagent kit (Zymo Research, Cat# 2051). RNA concentrations were measured using a NanoDrop spectrophotometer (Thermo Fisher). 1 ug of RNA was used to generate cDNA using iScript Reverse Transcription Supermix (Bio-Rad, Cat# 1708841). An Eppendorf Mastercycler Nexus Thermal Cycler (Millipore Sigma, Cat# EP6334000026) was used to generate cDNA. Quadruplicate biological samples were prepared in technical triplicates in a 96-well RT-qPCR plates (Bio-Rad, Cat#HSP9631). Primers were designed and purchased from Integrated Data Technologies. Primers are as follows: human *CDKN1A (p21)* (F: 5'-AGGTGGACCTGGAGACTCTCAG-3'; R: 5'-TCCTCTTGGAGAAGATCAGCCG-3'), human *INPP5D* (F: 5'- TGTGACCGAGTCCTCTGGAAGT-3'; R: 5'- GCCTCAAATGTGGCAAAGACAGG-3') and human *ACTINB* (F: 5'-CACCATTGGCAATGAGCGGTTC-3'; R: 5'-AGGTCTTTGCGGATGTCCACGT-3'). *ACTINB* mRNA expression levels were used as the internal control. Expression levels were expressed using the double delta cq method. Graphs were constructed using PRISM 10 Graphpad software.

RNA-sequencing and analysis

UM-SCC-47 and UPCI-SCC-90 cells were seeded at 300,000 cells per well in 6-well plates. After 24 hours, cells were transfected with either p53-targeting siRNA (Horizon Discovery, L-003329-00-0005) or

a non-targeting control (Horizon Discovery, D-001810-10-20) using Lipofectamine RNAiMAX (Thermo Fisher, 13778075). Cells were harvested 30 hours post-transfection, and RNA was extracted using the Direct-zol RNA MiniPrep with TRI Reagent kit (Zymo Research, Cat#2051). RNA concentrations were measured with a NanoDrop spectrophotometer (Thermo Fisher) and sent to Novogene for sequencing (Illumina PE150, 20M paired reads). Bioinformatic analysis was performed by Novogene using the DESeq2 software package for differential gene expression analysis. Genes with p-values < 0.01 were considered significant, regardless of q-values. Volcano plots were generated in RStudio.

FASTQ RNA-seq data files from isogenic PCI-13 p53WT and PCI-13 p53G245D cells were provided by Dr. Jeffrey N. Myers (The University of Texas MD Anderson Cancer Center) under a Material Transfer Agreement. Reads were aligned using the nf-core/RNAseq pipeline in paired-end mode and normalized read counts were generated and analyzed in R using limma, edgeR, and voom.

Human HNSCC tumor data

All data related to human HNSCC tumors including survival, gene expression, gene methylation, and chromosomal abnormalities, was obtained from cBioPortal using the TCGA PanCancer Atlas dataset.

Pathway Enrichment Analysis

We used the Gene Set Enrichment Analysis (GSEA) online tool to identify significantly enriched pathways in differentially expressed or differentially methylated genes. Enrichment analysis was performed using MSigDB GOBP, Reactome, and Wikipathways gene sets, with statistical significance determined by FDR q-value < 0.05.

Statistical analysis

Most data were analyzed using GraphPad Prism version 10. For cell line experiments, comparisons between two groups were performed using Student's t-test. Human tumor data comparisons were

conducted using the Mann-Whitney U test (Wilcoxon rank-sum test). Survival analysis was performed using the log-rank test (Mantel-Cox test). A p-value < 0.05 was considered statistically significant.

Author Contributions

J.G-A. conceptualized the study and performed experimentation, data analysis, and writing of original manuscript. H.L. contributed to experimentation. L.C.W. contributed to experimentation and writing of original manuscript. A.A.B. conducted bioinformatic analysis of RNA-seq files. J.N.M. provided cell lines and RNA-sequencing data. D.E.J and J.R.G, supervised, secured funding, edited original manuscript.

Acknowledgements

Schematics in Figure 4 and Supplementary Figure 1 were created using BioRender. J.G.-A. is supported by a University of California President's Postdoctoral Fellowship and a Pew Foundation Fellowship.

Supplemental Figures

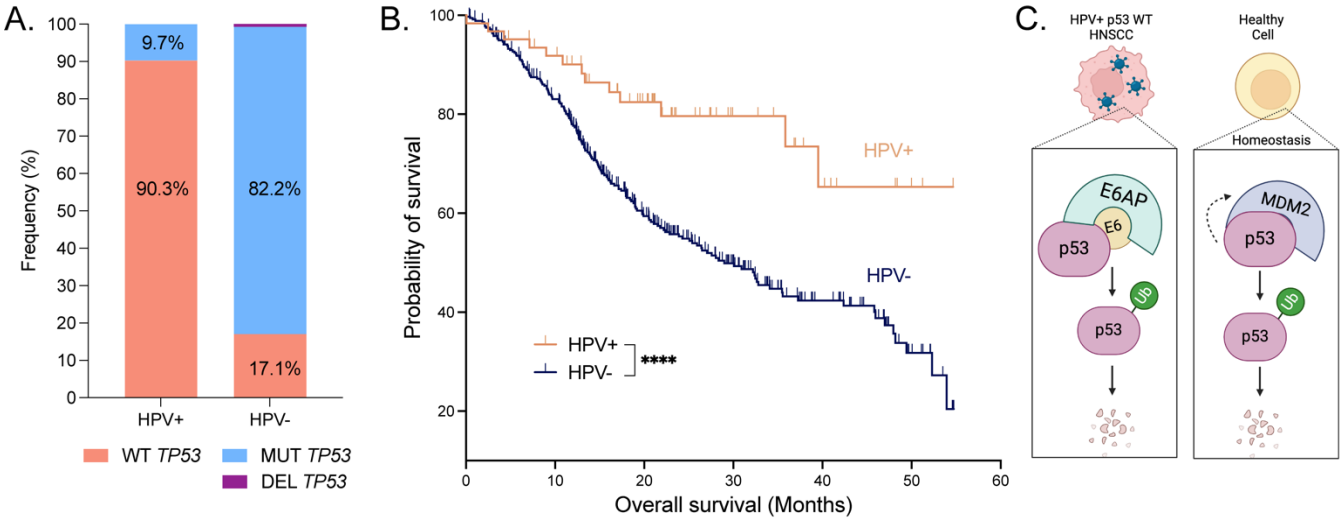

Supplemental Figure 1.- HPV+ HNSCC: Survival, *TP53* status, and parallels to physiological p53 regulation. A. Frequency of p53 (*TP53*) alterations in HNSCC. MUT=mutant, DEL=deleted. **B.** Overall survival comparison between HPV-positive (HPV+) and HPV-negative (HPV-) HNSCC. Data in A and B obtained from The Cancer Genome Atlas (TCGA, cBioPortal). ****p<0.00005. **C.** Diagram illustrating the molecular parallels between HPV-mediated p53 degradation and MDM2-mediated p53 degradation.

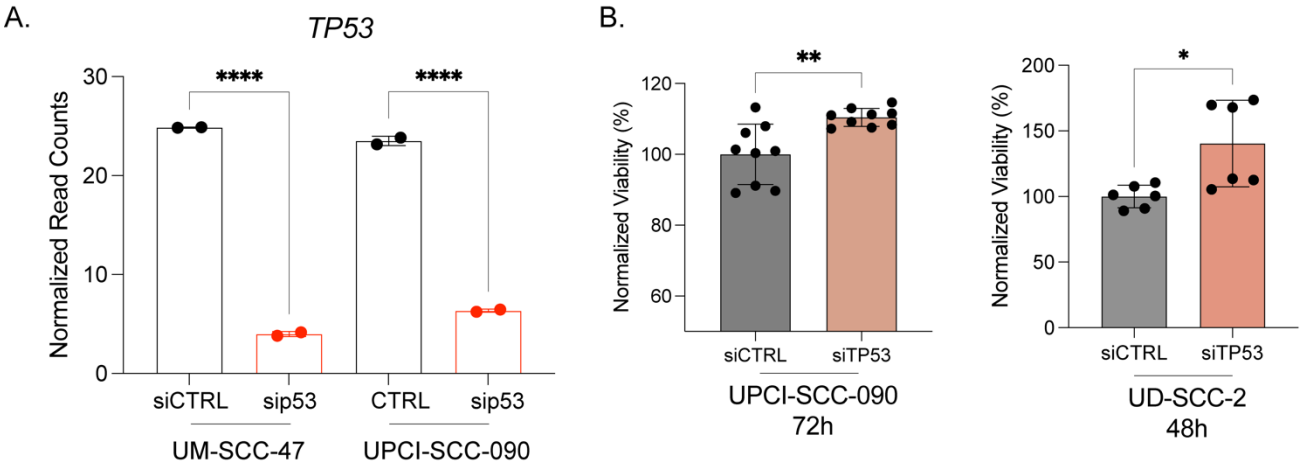

Supplemental Figure 2.- *TP53* mRNA levels following p53 knockdown and proliferation assessment. A. TP53 mRNA levels in UM-SCC-47 and UPCI-SCC-090 cells transfected with either non-targeting siRNA (siCTRL) or siRNA targeting p53 (sip53). RNA was collected 30 hours post-transfection, and RNA sequencing analysis was performed. Data are presented as normalized read counts. **B.** Viability assays following p53 knockdown (72 hours for UPCI-SCC-090; 48 hours for UD-SCC-2). Data are normalized to siCTRL and plotted as mean ± SEM. Statistical significance: *p < 0.05, **p < 0.005, ****p < 0.00005.

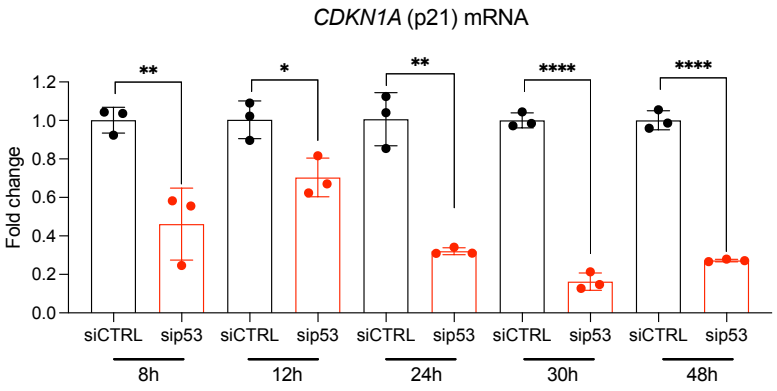

Supplemental Figure 3.- *CDKN1A* mRNA levels following p53 knockdown. UM-SCC-47 cells were transfected with either non-targeting siRNA (siCTRL) or siRNA targeting p53 (sip53). RNA was collected at 8, 12, 24, 30, and 48 hours post-transfection. qPCR analysis was performed to quantify *CDKN1A* mRNA levels, normalized to *ACTB* and expressed relative to siCTRL. Data are plotted as mean ± SEM. Statistical significance: *p < 0.05, **p < 0.005, ****p < 0.00005.

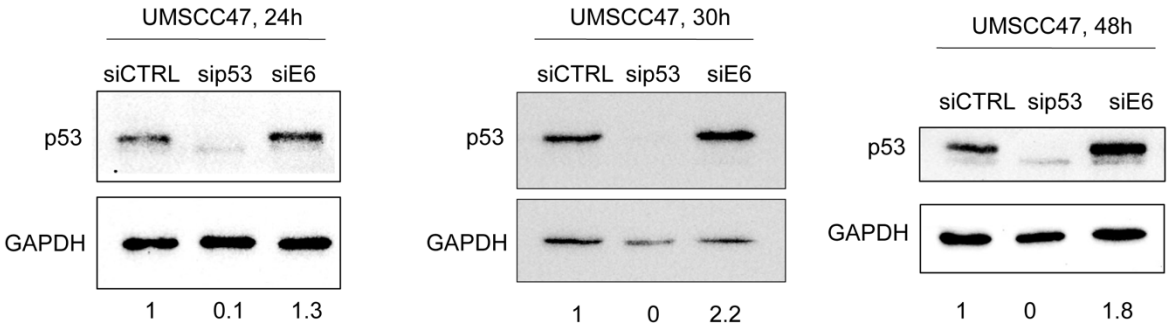

Supplemental Figure 4.- p53 protein levels following p53 or E6 knockdown. UM-SCC-47 cells were transfected with either non-targeting siRNA (siCTRL), siRNA targeting p53 (sip53), or siRNA targeting E6 (siE6). Cell pellets were collected at 24, 30, and 48 hours post-transfection. Immunoblots display p53 and GAPDH protein levels, with quantifications below showing relative p53 protein levels, normalized to GAPDH (loading control) and expressed relative to siCTRL conditions. The upper band in each p53 blot represents the p53-specific signal.

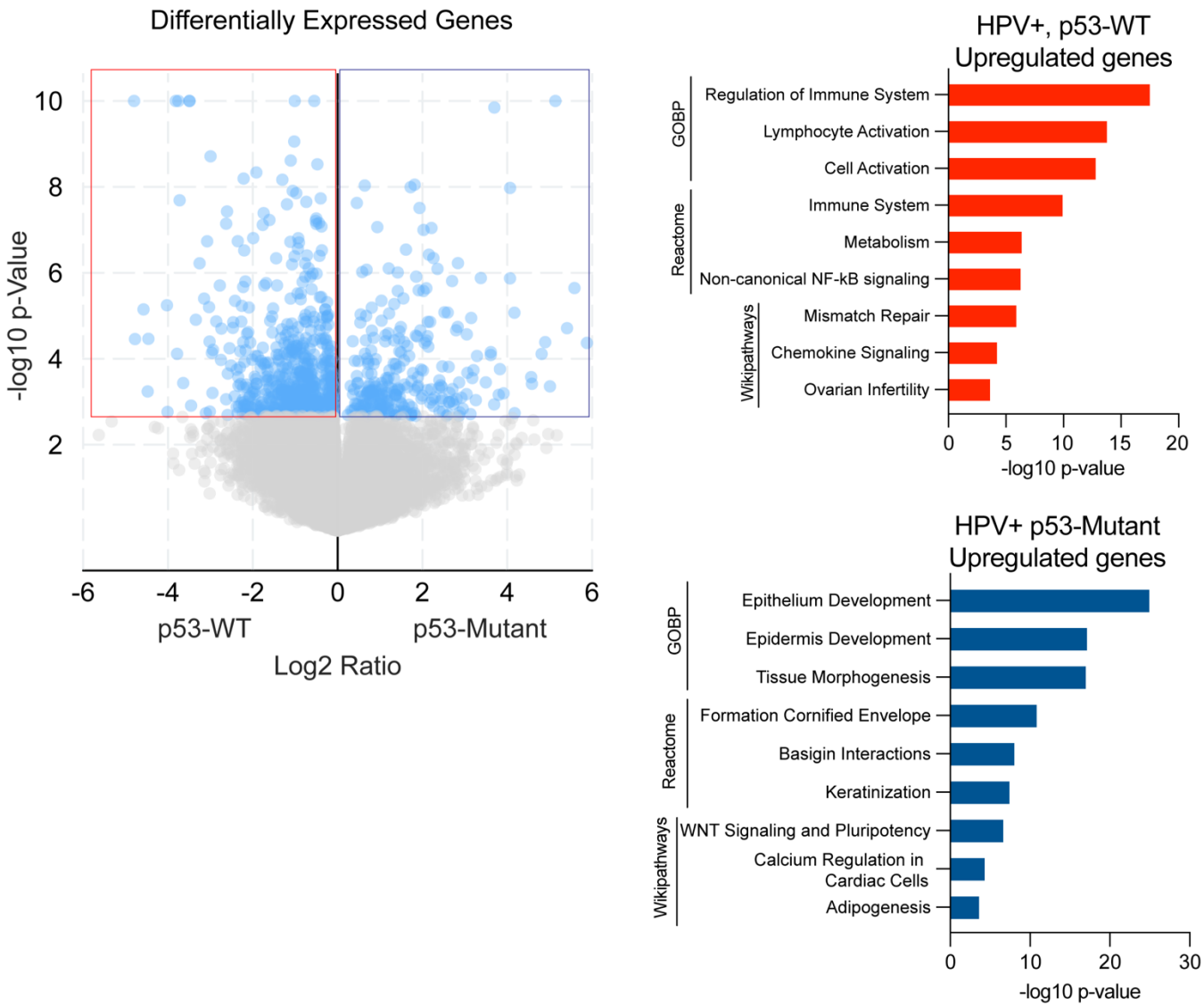

Supplemental Figure 5. Global transcriptomic differences between *TP53*-WT and *TP53*-Mutant HPV+ HNSCC tumors. Differential gene expression is presented as $\log_2$ fold change ($\log_2$Ratio). Significantly differentially expressed genes (DEGs) are highlighted in light blue in volcano plot. Red outline indicates genes significantly upregulated in *TP53*-WT tumors, while blue represents genes significantly upregulated in *TP53*-Mutant tumors. Right panels show pathway enrichment analysis of DEGs for each tumor type, with the top three significant pathways from three datasets plotted. Data extracted from TCGA (cBioPortal). GOBP=Gene Ontology Biological Process dataset.

References

1. Johnson, D.E., B. Burtness, C.R. Leemans, V.W.Y. Lui, J.E. Bauman, and J.R. Grandis, *Head and neck squamous cell carcinoma* (2020), 10.1038/s41572-020-00224-3
2. Cerami, E., J. Gao, U. Dogrusoz, B.E. Gross, S.O. Sumer, B.A. Aksoy, A. Jacobsen, C.J. Byrne, M.L. Heuer, E. Larsson, Y. Antipin, B. Reva, A.P. Goldberg, C. Sander, and N. Schultz, *The cBio cancer genomics portal: an open platform for exploring multidimensional cancer genomics data* (2012), 10.1158/2159-8290.CD-12-0095
3. Poeta, M.L., J. Manola, M.A. Goldwasser, A. Forastiere, N. Benoit, J.A. Califano, J.A. Ridge, J. Goodwin, D. Kenady, J. Saunders, W. Westra, D. Sidransky, and W.M. Koch, *TP53 mutations and survival in squamous-cell carcinoma of the head and neck* (2007), 10.1056/NEJMoa073770
4. Ang, K.K., J. Harris, R. Wheeler, R. Weber, D.I. Rosenthal, P.F. Nguyen-Tan, W.H. Westra, C.H. Chung, R.C. Jordan, C. Lu, H. Kim, R. Axelrod, C.C. Silverman, K.P. Redmond, and M.L. Gillison, *Human papillomavirus and survival of patients with oropharyngeal cancer* (2010), 10.1056/NEJMoa0912217
5. Gencel-Augusto, J. and G. Lozano, *p53 tetramerization: at the center of the dominant-negative effect of mutant p53* (2020), 10.1101/gad.340976.120
6. Wang, J.C.K., H.T. Baddock, A. Mafi, I.T. Foe, M. Bratkowski, T.Y. Lin, Z.D. Jensvold, M. Preciado Lopez, D. Stokoe, D. Eaton, Q. Hao, and A.H. Nile, *Structure of the p53 degradation complex from HPV16* (2024), 10.1038/s41467-024-45920-w
7. Pant, V. and G. Lozano, *Dissecting the p53-Mdm2 feedback loop in vivo: uncoupling the role in p53 stability and activity* (2014), 10.18632/oncotarget.1797
8. Montes de Oca Luna, R., D.S. Wagner, and G. Lozano, *Rescue of early embryonic lethality in mdm2-deficient mice by deletion of p53* (1995), 10.1038/378203a0

9. Zhang, Y., S. Xiong, Q. Li, S. Hu, M. Tashakori, C. Van Pelt, M.J. You, L. Pageon, and G. Lozano, *Tissue-specific and age-dependent effects of global Mdm2 loss* (2014), 10.1002/path.4368

10. Kon, N., M. Churchill, H. Li, S. Mukherjee, J.J. Manfredi, and W. Gu, *Robust p53 Stabilization Is Dispensable for Its Activation and Tumor Suppressor Function* (2021), 10.1158/0008-5472.CAN-20-1804

11. Boregowda, S.V., V. Krishnappa, J. Strivelli, C.L. Haga, C.N. Booker, and D.G. Phinney, *Basal p53 expression is indispensable for mesenchymal stem cell integrity* (2018), 10.1038/s41418-017-0004-4

12. McConnell, A.M., C. Yao, A.R. Yeckes, Y. Wang, A.S. Selvaggio, J. Tang, D.G. Kirsch, and B.R. Stripp, *p53 Regulates Progenitor Cell Quiescence and Differentiation in the Airway* (2016), 10.1016/j.celrep.2016.11.007

13. Garrido-Jimenez, S., J.F. Barrera-Lopez, S. Diaz-Chamorro, C.M. Mateos-Quiros, I. Rodriguez-Blanco, F.L. Marquez-Perez, M.J. Lorenzo, F. Centeno, A.C. Roman, and J.M. Carvajal-Gonzalez, *p53 regulation by MDM2 contributes to self-renewal and differentiation of basal stem cells in mouse and human airway epithelium* (2021), 10.1096/fj.202100638R

14. Gencel-Augusto, J., X. Su, Y. Qi, E.M. Whitley, V. Pant, S. Xiong, V. Shah, J. Lin, E. Perez, M.L. Fiorotto, I. Mahmud, A.K. Jain, P.L. Lorenzi, N.E. Navin, E.R. Richie, and G. Lozano, *Dimeric p53 Mutant Elicits Unique Tumor-Suppressive Activities through an Altered Metabolic Program* (2023), 10.1158/2159-8290.CD-22-0872

15. Labuschagne, C.F., F. Zani, and K.H. Vousden, *Control of metabolism by p53 - Cancer and beyond* (2018), 10.1016/j.bbcan.2018.06.001

16. Kenzelmann Broz, D. and L.D. Attardi, *TRP53 activates a global autophagy program to promote tumor suppression* (2013), 10.4161/auto.25833

17. Beckerman, R. and C. Prives, *Transcriptional regulation by p53* (2010), 10.1101/cshperspect.a000935

18. Moyer, S.M., A.R. Wasylishen, Y. Qi, N. Fowlkes, X. Su, and G. Lozano, *p53 drives a transcriptional program that elicits a non-cell-autonomous response and alters cell state in vivo* (2020), 10.1073/pnas.2008474117

19. Tsui, K.H., S.Y. Hsu, L.C. Chung, Y.H. Lin, T.H. Feng, T.Y. Lee, P.L. Chang, and H.H. Juang, *Growth differentiation factor-15: a p53- and demethylation-upregulating gene represses cell proliferation, invasion, and tumorigenesis in bladder carcinoma cells* (2015), 10.1038/srep12870

20. Backers, K., D. Blero, N. Paternotte, J. Zhang, and C. Erneux, *The termination of PI3K signalling by SHIP1 and SHIP2 inositol 5-phosphatases* (2003), 10.1016/s0065-2571(02)00043-2

21. Chang, J.W., D.K. Nomura, and B.F. Cravatt, *A potent and selective inhibitor of KIAA1363/AADACL1 that impairs prostate cancer pathogenesis* (2011), 10.1016/j.chembiol.2011.02.008

22. Rahman, M.A., A.R. Amin, D. Wang, L. Koenig, S. Nannapaneni, Z. Chen, Z. Wang, G. Sica, X. Deng, Z.G. Chen, and D.M. Shin, *RRM2 regulates Bcl-2 in head and neck and lung cancers: a potential target for cancer therapy* (2013), 10.1158/1078-0432.CCR-13-0073

23. Neskey, D.M., A.A. Osman, T.J. Ow, P. Katsonis, T. McDonald, S.C. Hicks, T.K. Hsu, C.R. Pickering, A. Ward, A. Patel, J.S. Yordy, H.D. Skinner, U. Giri, D. Sano, M.D. Story, B.M. Beadle, A.K. El-Naggar, M.S. Kies, W.N. William, C. Caulin, M. Frederick, M. Kimmel, J.N. Myers, and O. Lichtarge, *Evolutionary Action Score of TP53 Identifies High-Risk Mutations Associated with Decreased Survival and Increased Distant Metastases in Head and Neck Cancer* (2015), 10.1158/0008-5472.CAN-14-2735

24. Scheffner, M., B.A. Werness, J.M. Huibregtse, A.J. Levine, and P.M. Howley, *The E6 oncoprotein encoded by human papillomavirus types 16 and 18 promotes the degradation of p53* (1990), 10.1016/0092-8674(90)90409-8

25. Massimi, P. and L. Banks, *Repression of p53 transcriptional activity by the HPV E7 proteins* (1997), 10.1006/viro.1996.8315

26. Brand, T.M., S. Hartmann, N.E. Bhola, H. Li, Y. Zeng, R.A. O'Keefe, M.V. Ranall, S. Bandyopadhyay, M. Soucheray, N.J. Krogan, C. Kemp, U. Duvvuri, T. LaVallee, D.E. Johnson, M.A. Ozbun, J.E. Bauman, and J.R. Grandis, *Cross-talk Signaling between HER3 and HPV16 E6 and E7 Mediates Resistance to PI3K Inhibitors in Head and Neck Cancer* (2018), 10.1158/0008-5472.CAN-17-1672